

Looking at LTE in Practice

*A Performance Analysis of the
LTE System Based on Field Test Results*



Ayman Elnashar and
Mohamed A. El-Saidny

IMAGE LICENSED
BY INGRAM PUBLISHING

This article introduces a practical performance analysis of the long-term evolution (LTE) cellular system based on field test results from a commercially deployed Third-Generation Partnership Project's (3GPP's) Release 8 LTE network in Band-3 (i.e., 1,800 MHz, sometimes termed LTE1,800 MHz) with 20-MHz channel bandwidth. The presented analysis demonstrates the downlink (DL) and uplink (UL) throughputs in mobility conditions in addition to other aspects of the LTE system such as link budget, cell coverage, spectral efficiency, and handover performance. LTE's key features such as multiple-input, multiple-output (MIMO) and higher-order modulation [i.e., 64 quadrature amplitude modulation (QAM)] are assessed in different radio frequency (RF) conditions. A comparison is presented between LTE and 3GPP Release 8 evolution of high-speed packet access (HSPA+) with a dual-cell high-speed DL packet access (DC-HSDPA) feature based on the universal mobile telecommunications system (UMTS) 2,100-MHz commercial network with 10-MHz bandwidth (i.e., 2×5 -MHz adjacent carriers). The presented LTE network performance analysis and the comparison with the HSPA+ network can be used to benchmark the LTE

3GPP RELEASE 8 MARKS THE FIRST LTE DEPLOYMENT OF ORTHOGONAL FREQUENCY-DIVISION MULTIPLEXING AND MIMO TO INCREASE SPECTRAL EFFICIENCY.

system performance and evaluate the gains and merits of deploying the LTE network. It has been demonstrated that the LTE system outperforms the HSPA+ system in terms of spectrum efficiency, 64-QAM utilization, cell coverage, and handover delay. The LTE system offers a 34% improvement in spectrum efficiency, 40% 64-QAM utilization versus 7.4% for the HSPA+ system, and a 60% reduction in data interruption time during handover.

LTE System

The rapidly increasing number of mobile broadband users requires the availability of enhanced data services. The broadband traffic tsunami from applications, such as voice over IP (VoIP), high-quality and high-definition applications, online gaming, video sharing, true on-demand TV, and file loading, motivates an evolution in 3GPP broadband services. In addition, better coverage, higher capacity, robust quality of service (QoS), and lower latencies drive the next generation of 3GPP technologies. LTE aims to achieve these requirements.

3GPP Release 8 marks the first LTE deployment of orthogonal frequency-division multiplexing (OFDM) and MIMO to increase spectral efficiency. The benefits of LTE become possible with the introduction of the orthogonal frequency-division multiple access (OFDMA) on the DL and the single-carrier frequency-division multiple access (SC-FDMA) on the UL [1]. Both of these access schemes use OFDM, which is a form of frequency-division multiplexing (FDM), in which a large number of narrow-band, closely spaced subcarriers carry user data. The frequency spacing between the subcarriers maintains orthogonality between the subcarriers despite overlap and eliminates interference between the subcarriers [2]. This effectively eliminates the guard band requirement between the subcarriers that would be obligatory in a conventional FDM system. This approach achieves relatively high spectral efficiency and also eliminates the necessity of receiver filters for each subcarrier as needed in a conventional FDM system. Further benefits of OFDM include its robustness to multipath fading and the elimination of intersymbol interference (ISI) using a cyclic prefix (CP), as explained in [1].

Unlike legacy mobile technologies, LTE uses a variable channel bandwidth of 1.4, 5, 10, 15, or 20 MHz with an OFDMA in DL and an SC-FDMA in UL [3]. The subcarrier spacing is 15 kHz, although 7.5-kHz spacing is also defined for use with the multicast broadcast single-frequency network (MBSFN) mode of LTE. A short

and an extended CP are defined with 15-kHz subcarrier spacing with DL and UL, where seven or six OFDM symbols, respectively, are inserted into a slot of 0.5 ms. The longer CP, although more expensive in terms of overhead, enables successful deployment of LTE within a relatively large cell radius or where the delay spread is significantly higher than symbol duration, which can cause ISI. With regard to modulation schemes, quadrature phase-shift keying (QPSK), 16 QAM, and 64 QAM are all supported on both DL and UL with LTE based on the device capability [1]. Advanced antenna techniques such as single-user MIMO (SU-MIMO), multiple-user MIMO (MU-MIMO), and beamforming are supported in the DL to increase the peak data rates and average cell capacity [4]. In SU-MIMO, the focus of this article, the eNodeB (eNB) may transmit one or more streams to the same user to take advantage of capacity gains associated with the use of multiple transmit/receive antennas in rich scattering environments where channel variations can be tracked [5].

The 3GPP also introduced LTE Release 9, offering improvements to the throughput by introducing the heterogeneous network (HetNet) concept. Release 9 also introduced the voice over LTE and enhancements to circuit switch fallback (CSFB) to UMTS/Global System for Mobile Communications (GSM), which was initially introduced in Release 8 as an interim solution to support voice with LTE. Additionally, the 3GPP released LTE-Advanced, which is also referred to as *LTE Release 10 and beyond*. LTE-Advanced provides increased throughput and spectral efficiency by introducing carrier aggregation (CA) and higher-order MIMO, respectively. In addition, LTE-Advanced supports advanced interference management schemes such as enhanced interference cancellation, including enhanced intercell interference coordination (eICIC) and coordinated multipoint transmission (CoMP). It improves cell capacity and cell-edge throughput compared to Release 8 LTE.

The eNB provides the evolved UMTS terrestrial radio access (E-UTRA) user plane [packet data convergence protocol (PDCP) layer/radio link control (RLC) layer/medium access control (MAC) layer/physical (PHY) layer] and control plane [radio resource control (RRC) layer] protocol terminations toward the user equipment (UE). The eNBs connect by means of the standard (S1) interface to the evolved packet core (EPC), to the mobility management entity (MME) by means of the S1-MME, and to the serving gateway (S-GW) by means of the S1-U. The MME provides control plane signaling, security control, roaming and authentication, and radio bearer management. S-GW provides inter-radio access technology (inter-RAT) mobility, packet routing and forwarding, and transport level QoS mapping. The packet data network (PDN) gateway (P-GW) provides UE IP address allocation in addition to packet filtering and policy enforcement.

The radio interface protocol between UE and eNB consists of several layers. The physical layer of the LTE air interface performs functions such as coding, scrambling, modulation, transform precoding, and mapping to resource elements (REs) for OFDM procedures. Above this layer, the MAC layer handles the priority of logical channels and multiplexing of different logical channels. This mechanism supports negotiated QoS. The MAC layer also supports the hybrid automatic repeat request (HARQ) function to allow multiple and fast retransmissions for improved efficiency of the link. The RLC layer performs segmentation of packets to adapt the size of the transmitted packet to the data rate on the physical layer. Loss of a single segment can lead to retransmissions of multiple segments to recover packets. As a result, the RLC layer can also retransmit RLC packets. RLC status reports and, optionally, RLC automatic repeat request (ARQ) and MAC HARQ interactions determine the ARQ retransmissions. The PDCP processes control and user data. For user data, the PDCP layer performs header compression and ciphering. In addition, during handover, the PDCP can do in-sequence delivery and perform lossless handover. For control data, the PDCP layer provides a function for integrity protection.

The main focus of the LTE performance analysis in this article is the air interface protocol of the user plane and analysis of the handover on the control plane. As a result of the different mechanisms performed at the different layers, the total UL and DL throughputs will be maintained separately at each layer. For TCP/IP types of applications, Figure 1 shows the expected theoretical DL and UL throughputs of LTE for an LTE network, with configuration shown in Tables 1 and 2. The simulation results provide the DL/UL throughputs using the generalized protocol parameters specified in [3], [5], and [6]. It is worth mentioning that the end-user throughput is reflected by the application layer data rate (i.e., TCP/IP, in this example) and is impacted directly by the physical layer mechanisms and performance. The performance analysis described in this article is related to the physical layer of the LTE protocol stack.

In parallel with the LTE, 3GPP Release 8 introduced the dual-cell HS-DPA (DC-HSDPA) feature based on the legacy UMTS system (referred to as HSPA+). Using two adjacent DL carriers doubles the peak DL throughput compared to Release 7 with a single carrier and using 64 QAM. The DC-HSDPA allows aggregation of the two DL carriers for higher peak data rates of up to 42 Mb/s [7]. This also results

TABLE 1 General simulation parameters.

Configuration	DL	UL
LTE system bandwidth	20 MHz	20 MHz
UE category	3	3
Number of transport blocks	2 (MIMO 2 × 2)	1 (MIMO not configured but 2Rx are used on UL)
Maximum TBS (bits)	51,024	51,024
Physical layer BLER target	10%	10%
User physical layer scheduling rate	100%	100%

TABLE 2 Protocol layer inputs used for UL and DL throughput simulations.

Layer	UL and DL Overheads for One TBS
MAC headers	8 b
Total RLC headers	67 b with 0% retransmission rate
PDCP headers	68 b
TCP/IP headers	1,768 b

in reduced latency and higher cell capacity. Specifically, better trunking efficiency with joint scheduling of radio resources over two frequency carriers improves the cell capacity. Release 8 DC-HSDPA allows higher-order modulation with 64 QAM on both carriers, but Release 9 introduces the MIMO with the DC-HSDPA to allow for peak

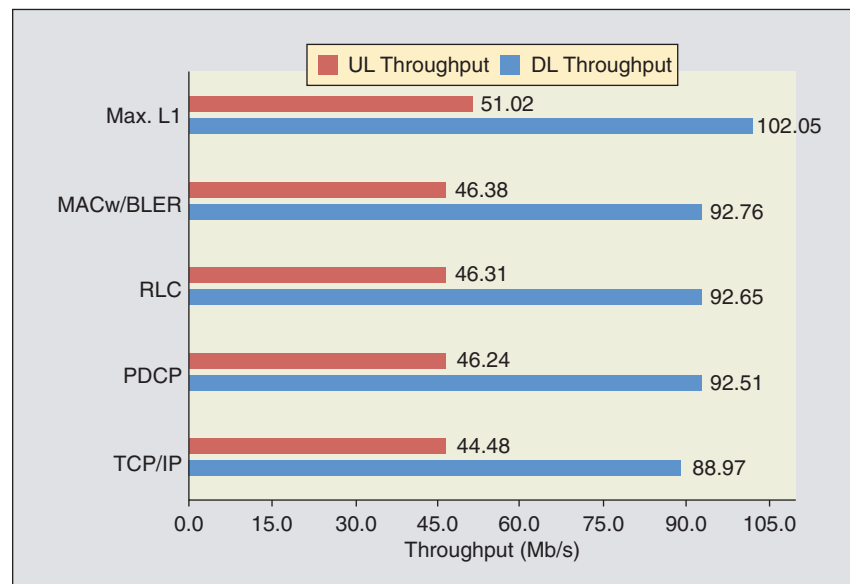


FIGURE 1 Theoretical LTE UL and DL throughputs.

throughput of 84 Mb/s. This article does not analyze Release 9 since the feature is not deployed in commercial networks, and the terminal is not yet available.

Test Environment

This section highlights the test environment and RF conditions for both the HSPA+ and the LTE network with the parameters highlighted in Table 1. The performance testing used colocated (i.e., the same physical sites are used) LTE/HSPA+ commercial networks. Several LTE performance analyses reported in [8]–[10] used simulation, trial sites, and/or limited testing environments. This article analyzes full commercial networks: LTE1,800 MHz with 20-MHz channel, referred to as *LTE network*, and UMTS2,100 with DC-HSDPA using 2×5 -MHz adjacent carriers, referred to as the *HSPA+ network*. A commercial LTE Category 3 (CAT3) data terminal connects to a laptop with logging and tracing tools. The same LTE CAT3 terminal supports the HSPA+ CAT24 mode for the HSPA+ performance analysis. For LTE, the terminal supports 100 Mb/s on DL and 50 Mb/s on UL with 2×2 MIMO and 64 QAM on DL and 16 QAM on UL. For HSPA+ Category 24, the terminal supports a maximum physical layer throughput of 42 Mb/s on DL and 5.76 Mb/s on UL (assuming UL Category 6 is used, which is a separate category for HSUPA). The terminal supports 64 QAM in DL on both carriers without MIMO.

The drive test route covers about 35 km with an urban morphology, referred to as the *mobility route*. The drive tests occurred at a speed of 80 km/h and were performed one at a time because the LTE and the HSPA+ networks share the same backhaul. Also, the testing occurred at a low traffic time with the two networks optimized for a rational benchmarking. The HSPA+ network used 40-W output power (i.e., each carrier is 40 W), whereas the LTE network used 60 W per antenna branch (2×60 W with MIMO 2×2). The configured DL primary common pilot physical channel (P-CPICH) power of the HSPA+ Node-B used 33 dBm, whereas the configured reference signal power (RSP) of the LTE eNB used 18 dBm.

Several UE-based measurements are used to quantify the RF conditions of the cells in the route. For LTE, the linear average over the power contributions (in watts) of the REs that carry cell-specific reference signals within the considered measurement frequency bandwidth define the measured reference signal received power (RSRP) [6]. The reference signal received quality (RSRQ) is defined as follows [6]:

$$\text{RSRQ} = \frac{N \cdot \text{RSRP}}{\text{RSSI}}, \quad (1)$$

where N is the number of resource blocks (RBs) of the E-UTRA carrier and RSSI is the received signal strength indication in the measurement bandwidth. The measurements in the numerator and denominator of (1) shall be made over the same set of RBs [6]. In addition, similar

to the UMTS concept, the channel quality indicator (CQI) is used to estimate the DL channel quality and used in dynamic scheduling on the DL. The CQI can be derived from RSRQ with UE reporting the best modulation and coding scheme (MCS) that can be decoded with block error rate (BLER) of $< 10\%$ [5]. The CQI effectively represents the modulation and coding that UE can support in the current RF conditions.

In addition to these measurements, assuming a receiver with two antennas, the 3GPP specification defines the signal-to-noise ratio (SNR) as follows [3]:

$$\text{SNR} = \frac{\hat{E}_s^{(1)} + \hat{E}_s^{(2)}}{N_{oc}^{(1)} + N_{oc}^{(2)}}, \quad (2)$$

where $\hat{E}_s^{(1)}$ [the superscript (1) indicates the receiver antenna number] is the received energy per RE (which consists of one subcarrier and one OFDM symbol) during the useful part of the symbol (i.e., excluding the CP) and averaged across the allocated RBs [average power within the allocated RB(s) is divided by the number of REs within this allocation, and normalized to the subcarrier spacing] at the UE antenna connector. $N_{oc}^{(1)}$ is the power spectral density (PSD) of a white-noise source (mean power per RE normalized to the subcarrier spacing), as measured at the UE antenna connector. The relationship between RB and RE is defined as follows [12]:

$$\text{RB} = N_{\text{symb}}^{\text{DL}} N_{\text{SC}}^{\text{RB}} \text{RE}, \quad (3)$$

where $N_{\text{symb}}^{\text{DL}}$ is the number of modulation symbols in the DL, and $N_{\text{SC}}^{\text{RB}}$ is the number of subcarriers per RB. More important is the signal-to-interference-plus-noise ratio (SINR), which is defined as the ratio of the average received modulated carrier power to the sum of the average cochannel interference power and the noise power from other sources.

On the HSPA+ side, the received signal code power (RSCP) and the CQI are adopted to represent the RF conditions of the HSPA+ network. Table 3 summarizes the key RF conditions components of LTE and HSPA+ in the mobility route. As shown in Table 3, both the LTE and HSPA+ exhibit good RF conditions.

TABLE 3 RF conditions comparison for LTE and HSPA+ systems.

LTE RF Measurements	Average Values
Serving cell RSRP (dBm)	-86.0
Serving cell RSRQ (dB)	-6.7
SINR (dB)	13.9
Wideband CQI (-)	9.0
HSPA+ RF Measurements	
RSCP (dBm)	-75.0
CQI (-)	20.0

The supported efficiencies of the two systems can be used based on the CQI measurements to benchmark the measured RF conditions between the two systems. While the reported CQI indices for both LTE and HSPA+ differ, the relationship between the CQI index and the efficiency can be used as an indicator to compare the RF conditions. The efficiency is defined in the context of modulation and coding rate. More specifically, the reported CQI by the UE corresponds to the supportable modulation and coding rate (i.e., spectral efficiency in bits/second/hertz) that it can receive with a transport block error probability of less than 10%. For HSPA+, it is derived based on the coding rate for each CQI, while for LTE, the mapping table is available in [5]. In both the systems, higher efficiency would engender a higher-order modulation and a higher coding rate. As provided in the 3GPP standard [5], the LTE efficiency of each CQI index is demonstrated in Figure 2. Similarly for HSPA+ and as per the 3GPP standard [13], [14], the efficiency derived from the CQI index is shown in Figure 2.

Figure 2 indicates that the practical estimated average CQI indices for both the LTE and HSPA+ systems (measured as 9 and 20, respectively) yield the same average efficiency, about 2.4 b/s/Hz. Therefore, it is evident that the RF conditions and power distributions for data channels for both the systems are very close, which yields a rational field benchmarking.

Coverage Analysis

LTE Link Budget Analysis

In this section, we provide practical field analysis to the link budget (LB) to validate the simulated throughputs.

The LTE LB quantifies the maximum allowable path loss (MAPL) between the transmitter and receiver. The LB determines the power and the noise levels between the transmitter and the receiver. It takes into account all the gain and loss factors occurring at different interfaces in the system. The LB provides the required SINR operating point associated with a specific BLER target. The expected data rate at the cell edge determines the critical coverage constraint when designing an LTE network. As a result, the cell-edge throughput specification determines the required SINR to meet such a requirement. For practical analysis of LB, mainly the following inputs factor into the estimate: SINR, system bandwidth, and antenna configuration at the eNB and the UE. The link curve, usually obtained via system-level simulations, maps the SINR to efficiency and forms a secondary input to LB analysis. The outcome of the LB calculations enables the network designer to determine the expected coverage calculated in theory and compare it with the measured values in the field. Figure 3 illustrates the measured SINR as a function of the measured path loss and also provides the relationship that determines the reported CQI from the measured SINR in the mobility route to validate the link budget and associated data rate at the cell edge.

To predict the network performance, each measured SINR value corresponds to a reported CQI to quantify the impact of the targeted SINR on the cell-edge data rate and on the maximum achievable path loss. From this estimation, the LB determines the number of cells required to fulfill the network coverage requirements. Figure 3 demonstrates that the lowest achieved path loss was 75 dB

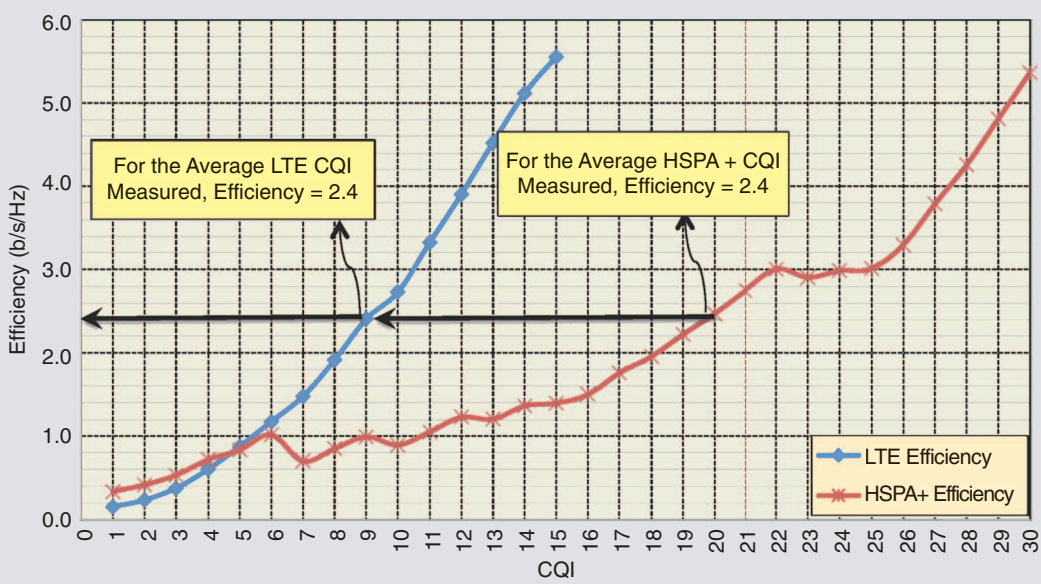


FIGURE 2 The efficiencies of LTE and HSPA+ systems as a function of CQI.

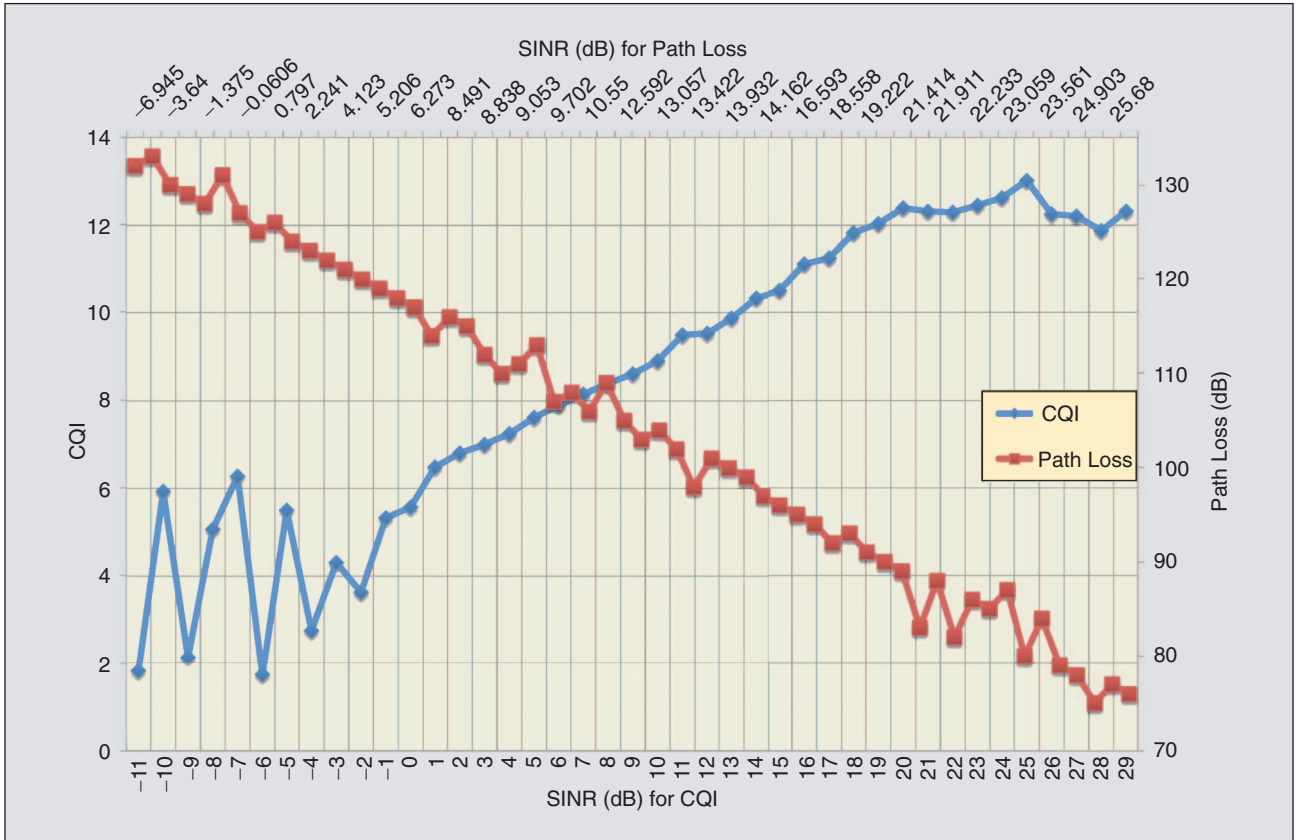


FIGURE 3 The measured SINR versus path loss and the reported CQI from the field measurements with trend lines.

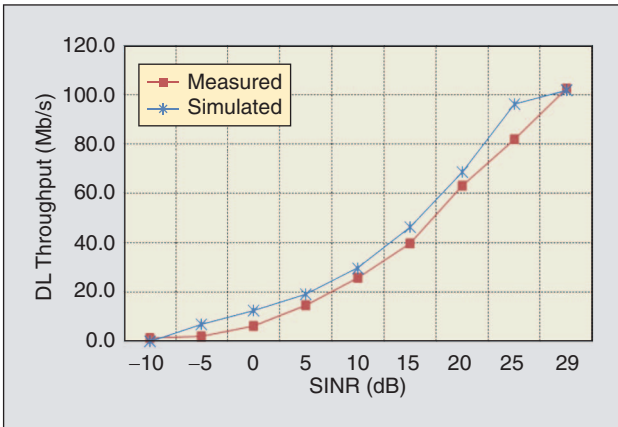


FIGURE 4 DL throughputs versus SINR for the field measurement results and simulation results.

at an SINR of about 25 dB, and the measured path loss increased up to 134 dB, while the SINR values deteriorated below -5 dB. More interestingly, Figure 3 indicates that the SINR has a linear relationship with the path loss. This linear relationship occurs because of the light load on the LTE network in terms of the number of connected users; intercell interference causes this relationship to deviate from linearity with a loaded LTE network. Also, the SINR has linear relationship with the CQI; therefore, the UL

and DL performance should change with path loss in the same fashion, as will be demonstrated in this section.

In LTE-connected mode (CM), the achieved SINR defines coverage instead of the reference signal level, as the reference signal mainly determines the CQI and MIMO rank indicator (RI) estimation. Figure 4 shows the normalized measured DL throughput as a function of SINR compared to the simulated values. A system-level simulator generates the simulated throughput. The 3GPP standard TS36.942 [15] provides a methodology for evaluating an LTE system, which is used here to estimate the simulated result in Figure 4. The modeled channel types considered in the standard may not necessarily represent the expected user conditions in an actual deployment, but the curves validate the field test results. Figure 4 demonstrates that the measured throughput corresponds closely with the simulated throughput.

Figure 5 shows the averages of UL and DL throughputs for each measured path loss during the mobility route. The path loss value in general is given by [5]

$$PL = RSP - RSRP, \quad (4)$$

where PL is the path loss, RSP is the provided RSP by higher layer, and RSRP is the higher layer filtered RSRP measured at the UE side. Figure 5 illustrates that the UL starts

to reach the targeted UL rate of 512 kb/s (the typical setting of the expected UL data rate at the cell edge) with the path loss of 130 dB (i.e., at RSRP = -112 dBm), whereas the DL starts to reach the targeted DL rate of 4.0 Mb/s (typical setting of the expected DL data rate at the cell edge) with the path loss of 130 dB. The estimated limiting link (DL/UL) can be derived from the following relationship:

$$\text{MAPL} = \text{Min}(\text{MAPL}_{\text{DL}}, \text{MAPL}_{\text{UL}}). \quad (5)$$

As a result, Figure 5 establishes the UL as the limiting link in the LTE system with MAPL of 4 dB less than the DL MAPL at the same throughput. In practice, determining the limiting link (DL or UL) based on MAPLs helps to estimate the cell radius per morphology, and therefore, the number of sites required to achieve the network coverage requirements.

Coverage Comparison Between LTE and HSPA+

A valid propagation model for a specific frequency and a specific morphology, for example, dense urban, urban, suburban, or rural, provide the relationship between the MAPL and the cell range and therefore a general approach to estimate the cell range. From the field results, with the same network configurations as in Table 1, the cell coverage of the LTE system is about 28% larger than the HSPA+ cell coverage, as clarified in Table 4. The cell coverage is estimated from the total serving cell changes (more accurately for LTE, it is the handover rate) observed for both the LTE network and the HSPA+ network over the entire mobility route with the related handover parameters for each technology. The difference in cell coverage is not only due to the frequency band, LTE at 1,800 MHz versus the HSPA+ at 2,100 MHz, and their associated propagation characteristics, but also to the system loading, which has a significant impact on the HSPA+ network.

Throughput Analysis

DL Throughput Analysis

This section compares the DL throughput performance of the LTE and HSPA+ systems during mobility at an average speed of about 80 km/h in the same test environment as described in the “Test Environment” section. The average DL physical layer throughput is about 33 Mb/s, as shown in Figure 6, with instantaneous peaks of about 96 Mb/s. Moreover, the DL average throughput improves with the introduction of Category 4 (CAT4) UE, which supports a peak DL throughput of 150 Mb/s. There is no commercially available CAT4 UE at this time. The introduction of

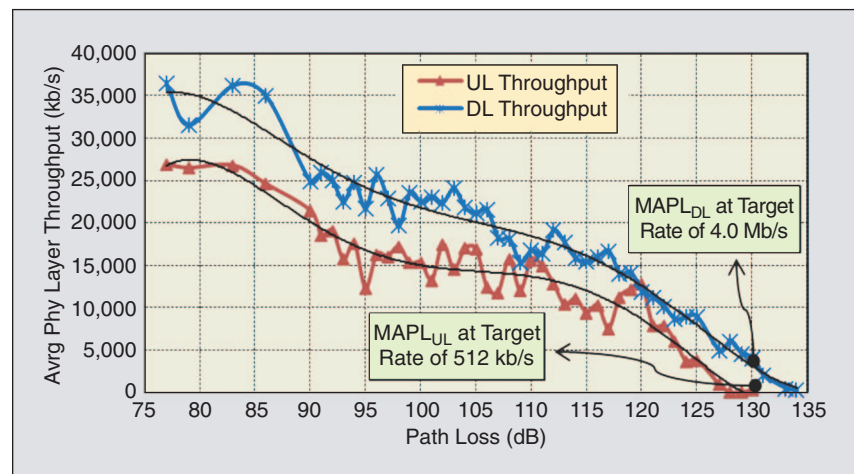


FIGURE 5 The LTE UL and DL throughput versus path loss.

CAT4 UE has no impact on the existing CAT3 UE, and the LTE network needs no software or hardware upgrade to support the CAT4 UE. The average DL HSPA+ throughput is about 9 Mb/s, with an instantaneous peak of 25 Mb/s. To compensate for the effect of loading in the HSPA+ network, normalized DL throughput is used to estimate the expected DL throughput of the unloaded HSPA+ network in the mobility route. Since the average network scheduling rate is 73%, estimated from the number of successful HS-SCCH decoded by the UE, the normalized average DL HSPA+ throughput is about 12.3 Mb/s, as shown in Figure 6. This estimate assumes a single user scheduled in the network under the RF conditions given in the “Test Environment” section. As a result, the average spectral efficiency of the LTE is 1.65, whereas it is 1.23 for the HSPA+ with a 34% improvement during the mobility conditions in this test route. The achieved average spectral efficiency based on the mobility test results is better than the baseline spectral efficiency estimated in [8] and substantially exceeds the target 1.53-b/s/Hz per sector in the DL set by the 3GPP at the start of the LTE design.

LTE UL Performance Analysis

This section analyzes the UL performance of the LTE system during mobility but excludes the HSPA+ network since there is no commercially available DC-HSUPA network, and therefore, the UL throughput will be on a single

TABLE 4 Serving cell change and cell radius comparison.

Measure	LTE	HSPA+
Drive route morphology	Urban	
Number of unique serving cells in the route	67 cells	100 cells
Mobility route (km)	39	39
Measured average coverage per cell (km)	0.50	0.39

THE TPC COMMANDS SENT BY ENB DYNAMICALLY ADJUST THE POWER DEPENDING ON THE REQUIRED BLER TARGET AND LINK QUALITY.

carrier. In addition to the LTE UL throughput, the UL transmit power is also evaluated. The average LTE UL throughput is about 14 Mb/s with an instantaneous peak of 50 Mb/s. Therefore, the average mobility spectral efficiency of the UL is 0.7. Moreover, the UL spectral efficiency will improve with the introduction of advanced interference-management schemes to improve the cell-edge throughput.

Figure 7 shows that during the entire mobility route, the UL BLER remained at 10% most of the time, while the UL

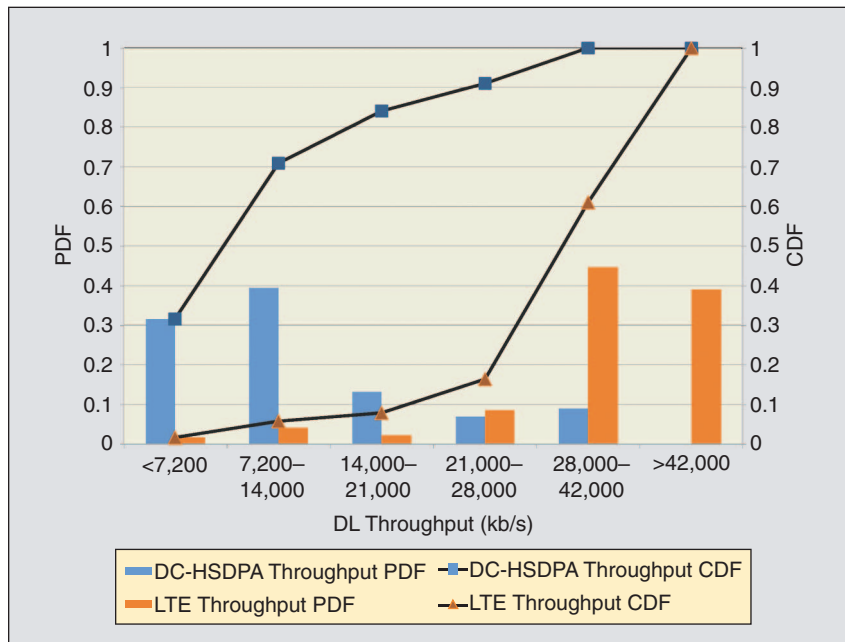


FIGURE 6 DL throughputs for DC-HSDPA and LTE.

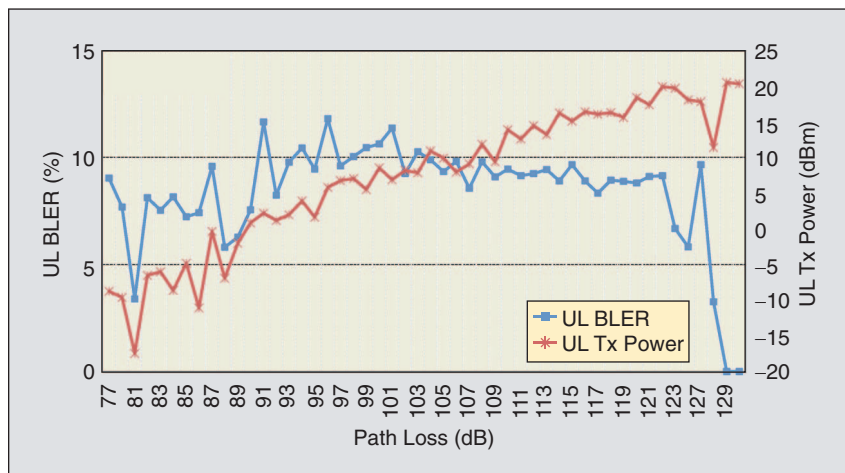


FIGURE 7 ULTx power and BLER in mobility route.

power increased based on the path loss and power control parameters. Figure 7 illustrates the UE UL power and UL BLER versus the path loss. The UL power exceeds 15 dBm at a path loss of 114 dB.

In code division multiple access (CDMA)-based systems, all users in the UL share the same frequency resources. As a result, the Node-B must manage the power of individual UEs so that each UE can maintain a specific level of link quality. In OFDMA systems, the individual UEs use different time-frequency resources for transmission. As a result, the intracell interference is less critical, but the intercell interference matters. The UL power control maintains a specific link quality level. Two mechanisms manage the LTE UL power control: open-loop power control (OLPC), which provides a basic operating point, and closed-loop power control (CLPC), which uses transmit power control (TPC) commands [7]. The TPC commands sent by eNB dynamically adjust the power, depending on the required BLER target and link quality.

Figure 8 illustrates the Tx power distributions per UL channel observed in the test route. Three UL channels contribute to the UE Tx power: the physical UL shared channel (PUSCH), which carries the UL user data, the sounding reference signal (SRS), which provides the UL channel quality estimation feedback, and the physical UL control channel (PUCCH), which carries control information. The total average UL Tx power observed in the test route is about 9.9 dBm for a UE with a power amplifier (PA) capable of 23 dBm, as shown in Figure 7.

The main contributor to the adjustments of the PUSCH power is the OLPC component. The UE's measured DL path loss and the configuration parameters mainly drive the UL power. This occurs because a typical scheduling mechanism tends to increase the data rate and hence the UE Tx power in a lightly loaded system, which maximizes the SINR and thus the UL throughput. Figure 8 depicts the total power distribution per UL channel in the test route. Figure 9 illustrates the PDF and CDF of the CLPC TPC commands, which indicate that the eNB scheduler merely requires the immediate adjustment of the UE power.

MIMO and 64-QAM

Performance Analysis

In this section, we analyze two key LTE features: MIMO and 64 QAM. 3GPP Release 8 supports several MIMO configurations. The MIMO usage can be one of the seven available transmission modes [5]. This study considers transmission mode 3 (TM3), which supports SU-MIMO that does not need the UE to report a pre-coding matrix indicator (PMI) and allows support of two code words and peak throughput in most suitable channel conditions. This technique suits high-mobility scenarios, where the overhead of the reporting PMI adds no value. However, this mode requires the UE to report the RI. With MIMO TM3 operation, either one or two code words of information can be sent. With MIMO Rank 1 (i.e., RI = 1), only a single code word of information is sent, whereas with Rank 2 (i.e., RI = 2), two code words are sent. The UE sends the preferred option through the RI, which can take the value of 1 or 2.

The UE requests Rank 1 or 2 according to the RF conditions. Specifically, in poor RF conditions, the UE would tend to request Rank 1, transmit diversity, where both the antenna ports send the same data streams. In good RF conditions, the UE would tend to request Rank 2, space diversity, where the two antenna ports send different data streams. Figure 10 demonstrates the average two-code-word usage as scheduled by the eNB in the mobility route as a function of the CQI. The two-code-word usage dominates in the entire mobility route, dropping to 50% at CQI = 8 and starting to diminish at CQI < 3. The usage of two code words in the route is about 62%. While in Rank 2, up to 100% MIMO occurs, assuming that both the streams have the same quality.

With regard to higher-order modulation, based on the reported CQI, the eNB scheduler selects the MCS assigned to the user. The 3GPP standard allows MCS indices of 0–31 [5]. The MCS range of 0–9 allows QPSK modulation, MCS 10–16 allows 16-QAM modulation, MCS 17–28 allows 64-QAM modulation usage, and the range of MCS 29–31 allows for special operation during retransmissions [3]. The UE derives the transport block size (TBS) in bits for each

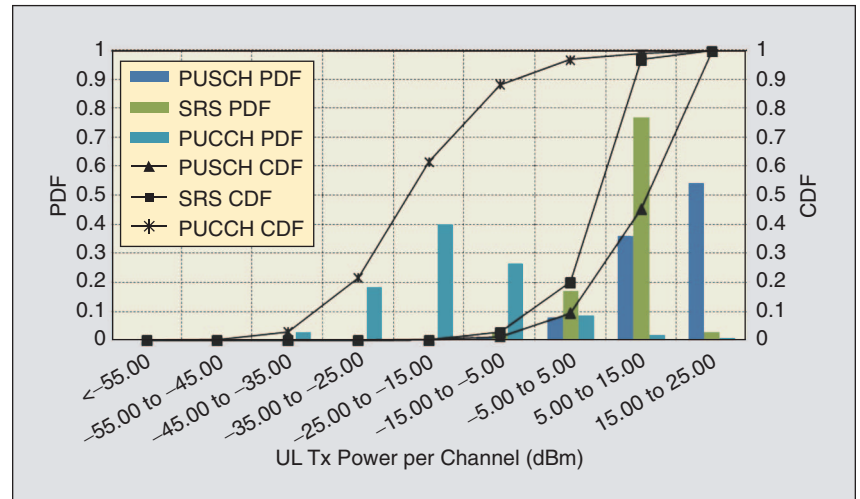


FIGURE 8 LTE UL Tx power per channels.

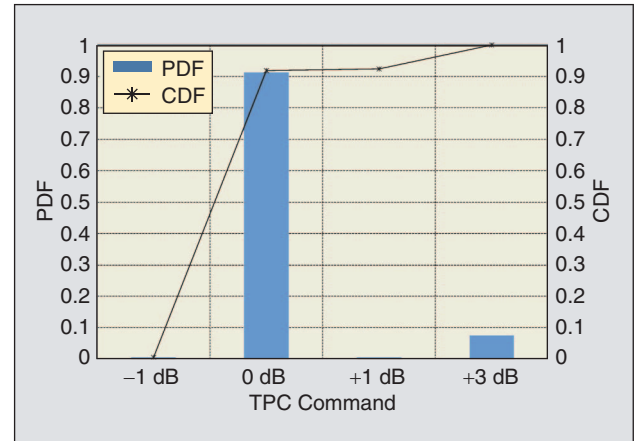


FIGURE 9 PUSCH TPC commands for CLPC.

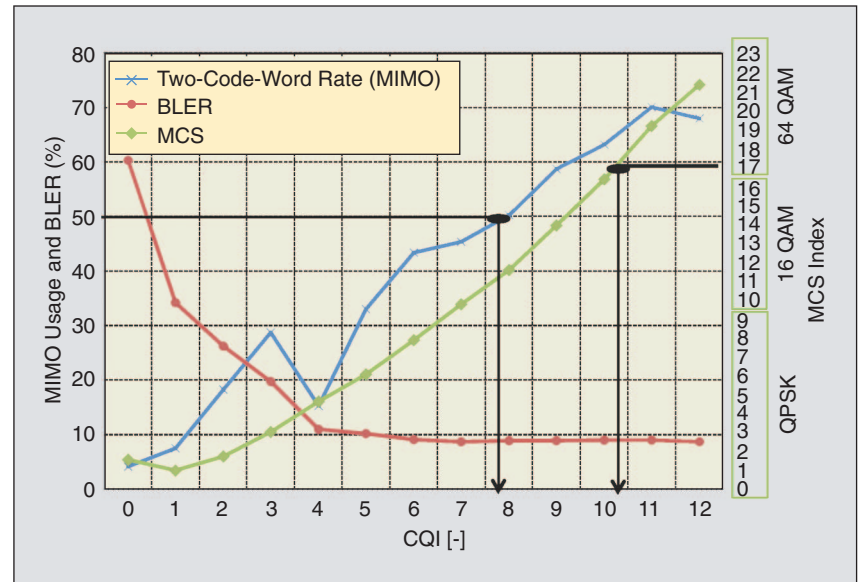


FIGURE 10 LTE MIMO, 64-QAM usage, and BLER as a function of CQI.

INTRAFREQUENCY HANDOVER PERFORMANCE IN THE MOBILITY ROUTE ILLUSTRATES THE KEY FACTORS IMPACTING DL THROUGHPUT AT THE CELL EDGE.

stream from the MCS. Figure 11 shows that 64-QAM usage is 40%, MCS ≥ 17 in the entire route dropping at CQI < 10 , as shown in Figure 10. The 3GPP standard expects 64-QAM usage for CQI = 10 to maintain the 10% BLER [5]. The test results in Figure 10 demonstrate a perfect match between the CQI and 64-QAM usage in the mobility route, while BLER is maintained at 10% for the entire range of CQI except at the edge of the coverage when CQI = 4.

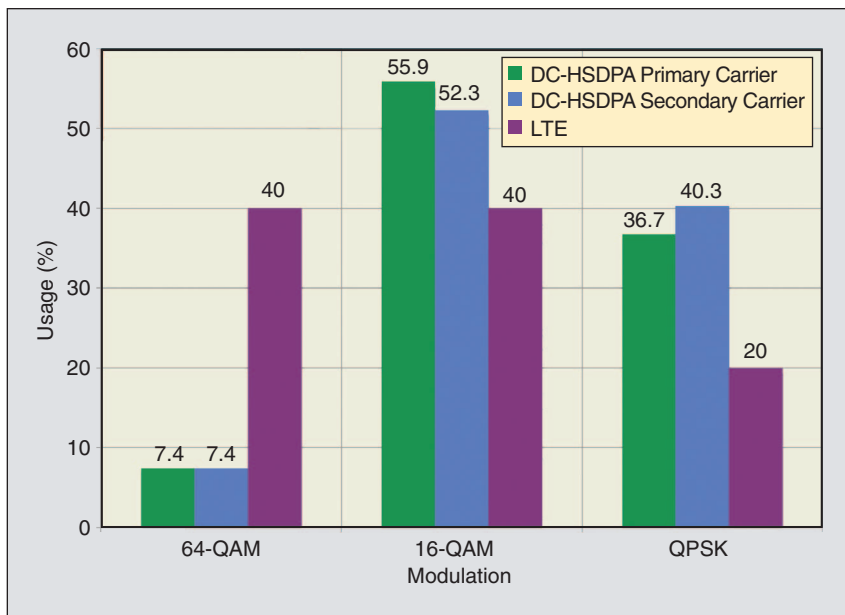


FIGURE 11 LTE and HSPA+ modulation usage in mobility route.

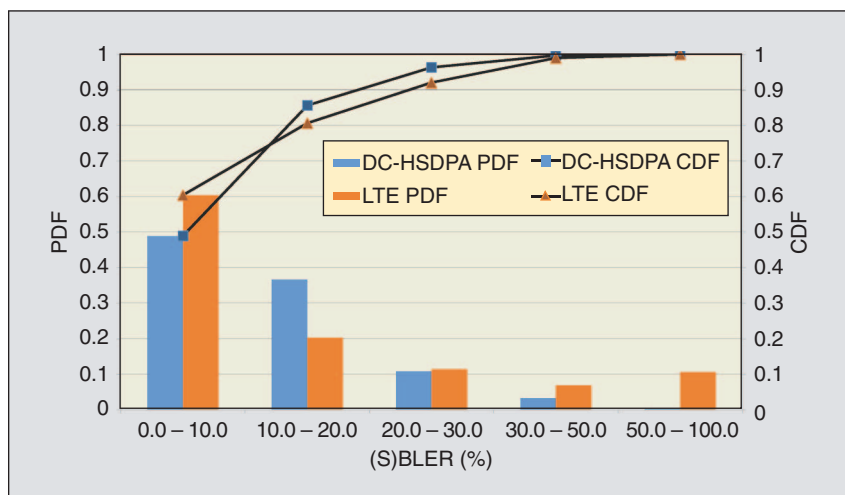


FIGURE 12 DL (S)BLER measurements for DC-HSDPA and LTE.

For HSPA+, 64-QAM usage is 7.4% per carrier in the entire route, as depicted in Figure 11. The 3GPP expects strong usage of 64 QAM at CQI = 25 [15]. Note that the measured CQI for each technology yields different coding rates and different spectral efficiencies.

Figure 12 demonstrates the HSPA+ subblock error rate (SBLER) and LTE DL BLER. The average SBLER of the HSPA+ system also remains at 10%, which yields the same impact on the end user total observed throughput.

Handover Performance

Intrafrequency handover performance in the mobility route illustrates the key factors impacting DL throughput at the cell edge. In the HSPA+, the radio network controller (RNC) still manages handover, whereas in

LTE Release 8, handovers occur through a direct interface between the eNBs. From an air interface perspective, the LTE handovers are all hard, meaning that the air interface connection with the source eNB breaks before connecting with the target eNB.

Figure 13 illustrates the handover procedure of LTE, analyzed in terms of average handover time and average DL data interruption time. The RRC layer of the control plane carries the message flow between the UE and the source and target eNBs. The RRC layer in general carries system information blocks (SIBs) broadcasting, measurement configurations, and mobility control in the connected and idle states, as well as system selection and reselection. For LTE X2-based handover, when UE sends a measurement report message over the RRC layer to the source eNB, the source eNB sends a handover request to the target eNB that includes a list of the bearers that will be transferred and possibly a DL data-forwarding proposal. Then, the source eNB sends an RRC connection reconfiguration message to the UE over the RRC layer, after which the source eNB forwards any pending DL packets to the target eNB. The UE then synchronizes with the target eNB using a random-access procedure, and once successful, the UE sends an RRC connection reconfiguration complete message over the newly

established RRC. The UE then starts collecting the SIBs, which carry the required information for the UE about the cell-level configuration parameters, from the target eNB. The target eNB sends a UE context release message to the source eNB, confirming the successful handover and enabling source eNB resources to be released.

The field results indicate that the average LTE X2-based handover time is about 30 ms, as demonstrated in Figure 14. The delay measured includes the total processing time taken and the air interface packet latencies needed to process the handover request sent by eNB. As for the LTE DL data interruption time, the average interruption time observed in the route is about 50 ms, as shown in Figure 13. The DL data interruption time is the period where the DL throughput stops during the serving cell change. The RLC packets received from the source and the target eNBs during the handover allow calculation of the interruption time.

Figure 15 demonstrates the data interruption time of the HSPA+ network in the same mobility route. The average interruption time is about 128 ms, which is also calculated at the RLC layer from the last and first packets received by the UE from the source and the target serving HSPA+ cells, respectively. As a result, the LTE X2-based handover offers a reduction of about 60% in terms of data interruption time. This gain directly improves the user experience in terms of the DL throughput during mobility conditions. This reduction comes mainly from the lower processing and lower round trip times (RTT) of the packets in LTE system. It is important to note that the HSPA+ system uses an unsynchronized serving cell change (USCC) procedure and does not implement the 3GPP Release 8 enhanced serving cell change (E-SCC), which should reduce the data interruption time of the HSPA+ network. Note that some vendors choose not to deploy this feature because of limited anticipated gain and lack of handsets that support this feature.

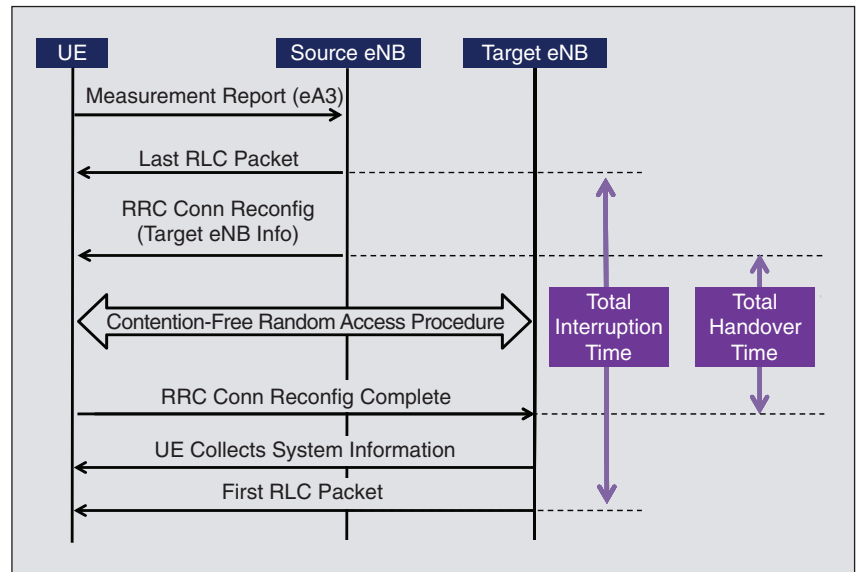


FIGURE 13 LTE handover measurements.

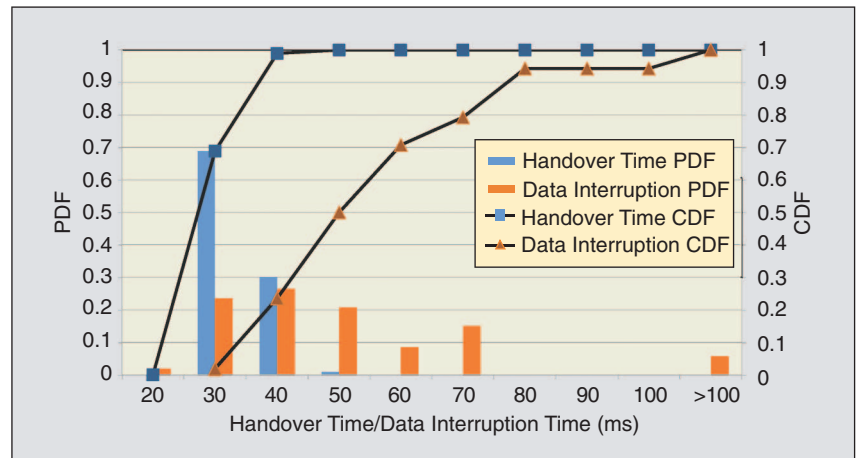


FIGURE 14 LTE handover delay and data interruption time.

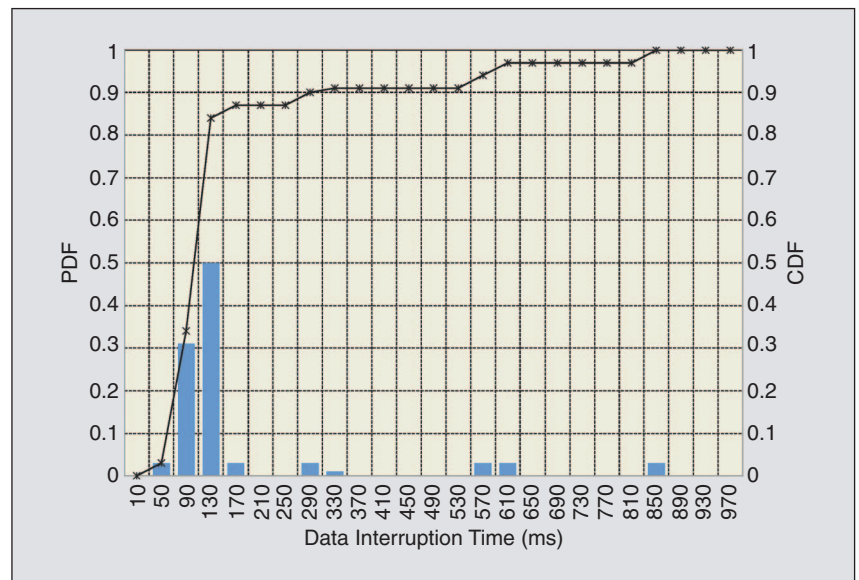


FIGURE 15 DC-HSDPA data interruption time.

Conclusions

In this article, we described a detailed practical performance analysis of the LTE cellular system based on field test measurements from a commercially deployed LTE network and a comparative analysis between LTE and HSPA+. We measured key performance metrics for both the LTE and HSPA+ systems, including RSRP, RSRQ, BLER, CQI, SINR, RSCP, and spectral efficiency. Both systems had similar measured RF conditions and power distributions, yielding a coherent field benchmarking. The UL and DL throughput performances vary in the same fashion with path loss due to the linear relationship between the SINR and CQI. Moreover, the actual DL throughput performance versus SINR matches the 3GPP simulation results. Unlike the HSPA+ system, the LTE system is UL limited, and therefore, fewer cells cover the same route. Furthermore, the mobility field results demonstrate that the LTE system offers a 34% improvement in spectral efficiency compared with HSPA+. MIMO with Rank 2 and 64 QAM occurred frequently along the mobility route with the usage of 62% and 40%, respectively. However, the HSPA+ system used 64 QAM for only 7.4%. Finally, the LTE system demonstrated reduced interruption time during handover of 50 ms compared with the 128-ms interruption time of the HSPA+ system during serving cell change, which improves the end-user experience. Future work may include performance analysis of CAT4 UE LTE terminals, DC-HSDPA with MIMO in 10 MHz, DC-HSUPA, and other HSPA+ performance-related features such as E-SCC. Also, performance analysis of the LTE system with different loading scenarios and the key features in 3GPP Release 9 and LTE-Advanced are potential topics for future work.

Author Information

Ayman Elnashar received the B.Sc. degree in electrical engineering (communications and electrophysics division) from Alexandria University, Egypt, in 1995 and the M.Sc. and Ph.D. degrees in electrical communications engineering from Mansoura University, Egypt, in 1999 and 2005, respectively. He has more than 16 years of practical experience in the telecoms industry, including GSM, GPRS/EDGE, and UMTS/HSPA+/LTE. Currently, he is senior director of wireless broadband and terminals with the Emirates Integrated Telecommunications Company “du,” United Arab Emirates. He is in charge of mobile and fixed wireless broadband networks and terminals testing and validation. Prior to this, he was with Mobily (Etisalat), KSA, from June 2005 to January 2008 and with MobiNil (orange), Egypt, from March 2000 to June 2005. He played key roles in contributing to the success of mobile broadband networks of Mobily/KSA and du/UAE. His research interests include performance analysis of cellular systems, mobile network

planning and design, digital signal processing for wireless communications, multiuser detection, smart antennas, beamforming, and adaptive detection.

Mohamed A. El-Saidny received the B.Sc. degree in computer engineering and the M.Sc. degree in electrical engineering from the University of Alabama, Huntsville, in 2002 and 2004, respectively. From 2004 to 2008, he was working in the CDMA technology division at QUALCOMM Inc., San Diego, California. He was responsible for performance evaluation and analysis of the Qualcomm UMTS system and software chipset solutions used in user equipment. Since 2008, he has been working in the Qualcomm Corporate Engineering Services division in Dubai, United Arab Emirates. His current specialties include system studies and design of 3G and 4G technologies: Release-99, HSPA(+), and LTE.

References

- [1] 3GPP, “3rd Generation Partnership Project; Technical specification group radio access network; Evolved universal terrestrial radio access (E-UTRA); LTE physical layer—general description,” TS 36.201 V8.3.0, 2009.
- [2] G. Berardinelli, L. Á. M. R. de Temiño, S. Frattasi, M. I. Rahman, and P. Mogensen, “OFDMA vs. SC-FDMA: Performance comparison in local area IMT-A scenarios,” *IEEE Wireless Commun.*, vol. 15, no. 5, pp. 1536–1546, Oct. 2008.
- [3] 3GPP, “3rd Generation Partnership Project; Technical specification group radio access network; Evolved universal terrestrial radio access (E-UTRA); User equipment (UE) radio transmission and reception,” TS 36.101, V8.15.0, 2011.
- [4] J. Lee, J.-K. Han, and J. Zhang, “MIMO technologies in 3GPP LTE and LTE-Advanced,” *EURASIP J. Wireless Commun. Networking*, vol. 2009, Article ID 302092, pp. 1–10.
- [5] 3GPP, “3rd Generation Partnership Project; Technical specification group radio access network; Evolved universal terrestrial radio access (E-UTRA); Physical layer procedures,” TS 36.213, V8.8.0, 2009.
- [6] 3GPP, “3rd Generation Partnership Project; Technical specification group radio access network; Evolved universal terrestrial radio access (E-UTRA); User equipment (UE) radio access capabilities,” TS 36.306, V8.8.0, 2011.
- [7] 3GPP, “3rd Generation Partnership Project; Technical specification group radio access network; UE radio access capabilities,” TS 25.306, V8.12.0, 2011.
- [8] R. Irmer, H.-P. Mayer, A. Weber, V. Braun, M. Schmidt, M. Ohm, N. Ahr, A. Zoch, C. Jandura, P. Marsch, and G. Fettweis, “Multisite field trial for LTE and advanced concepts,” *IEEE Commun. Mag.*, vol. 47, no. 2, pp. 92–98, Feb. 2009.
- [9] J. Robson, “The LTE/SAE trial initiative: Taking LTE/SAE from specification to rollout,” *IEEE Commun. Mag.*, vol. 47, no. 4, pp. 82–88, Apr. 2009.
- [10] G. Piro, L. A. Grieco, G. Boggia, F. Capozzi, and P. Camarda, “Simulating LTE cellular systems: An open-source framework,” *IEEE Trans. Veh. Technol.*, vol. 60, no. 2, pp. 498–513, Feb. 2011.
- [11] 3GPP, “3rd Generation Partnership Project; Technical specification group radio access network; Evolved universal terrestrial radio access (E-UTRA); Physical layer—measurements,” TS 36.214, V8.7.0, 2009.
- [12] 3GPP, “3rd Generation Partnership Project; Technical specification group radio access network; Evolved universal terrestrial radio access (E-UTRA); Physical channels and modulation,” TS 36.211, V8.9.0, 2009.
- [13] 3GPP, “3rd Generation Partnership Project; Technical specification group radio access network; Physical layer procedures (FDD),” TS 25.214, V8.12.0, 2011.
- [14] 3GPP, “3rd Generation Partnership Project; Technical specification group radio access network; Multiplexing and channel coding (FDD),” TS 25.212, V8.11.0, 2009.
- [15] 3GPP, “3rd Generation Partnership Project; Technical specification group radio access network; Evolved universal terrestrial radio access (E-UTRA); Radio frequency (RF) system scenarios,” TS 36.942, V8.3.0, 2010.